



LAWRENCE
LIVERMORE
NATIONAL
LABORATORY

LLNL-TR-865279

Milestone (ID#7453, Q2 FY24) report

K. Fournier

June 5, 2024

Disclaimer

This document was prepared as an account of work sponsored by an agency of the United States government. Neither the United States government nor Lawrence Livermore National Security, LLC, nor any of their employees makes any warranty, expressed or implied, or assumes any legal liability or responsibility for the accuracy, completeness, or usefulness of any information, apparatus, product, or process disclosed, or represents that its use would not infringe privately owned rights. Reference herein to any specific commercial product, process, or service by trade name, trademark, manufacturer, or otherwise does not necessarily constitute or imply its endorsement, recommendation, or favoring by the United States government or Lawrence Livermore National Security, LLC. The views and opinions of authors expressed herein do not necessarily state or reflect those of the United States government or Lawrence Livermore National Security, LLC, and shall not be used for advertising or product endorsement purposes.

This work performed under the auspices of the U.S. Department of Energy by Lawrence Livermore National Laboratory under Contract DE-AC52-07NA27344.

March 2024

NIF-1014896823

Milestone (ID#7453, Q2 FY24) report.

Title: Capability for time-resolved diffraction for material phase in extreme conditions

Completion Criteria: Demonstrate >3 frame diffraction diagnostic on a high-pressure material platform (FIDDLE)

Executive summary

After a series of development experiments, a new x-ray diffraction diagnostic called FIDDLE (Flexible Imaging Diffraction Diagnostic for Laser Experiments) has been designed, built, and fielded on four shots at NIF (Figure 1). Here we document the initial performance of FIDDLE fielded as the detector in the time-resolved x-ray diffraction experimental platform. Early challenges with EMP have been documented using offline testing in the Target Diagnostics Factory to identify EMP leaks. These techniques were used to guide the application of shielding to weak spots where EM radiation was able to penetrate inside the diagnostic. Application of shielding was found to be effective at reducing EMP leaks, enabling detection of x-ray diffraction on three temporally separated frames during a high pressure (~1Mbar) experiment where lead (Pb) was observed to undergo a phase transition from HCP to BCC.



Figure 1. New FIDDLE diagnostic: (left) during assembly; (center) during installation above the polar DIM; (right) during NIF shot N230727-001-999.

Background

Materials frequently undergo structural phase transitions when they are compressed, as the addition of thermodynamic energy changes the stability of bonding. Moreover, many extrinsic material properties, e.g., strength, thermal conductivity, and electrical conductivity, are directly related to the crystal structure. (The canonical example of this is carbon, with low-pressure graphite and high-pressure diamond having massively different properties.) Consequently, to predict material behavior at high pressures, it is important to understand the phase in addition to measuring the density and equation of state.

Experiments that use laser drive to achieve multi-megabar compression of materials have identified exciting new material phases in fundamental science [1] and produced important results relevant to the High Energy Density programs at LLNL and other national laboratories. [2] X-ray diffraction is a critical tool in these experiments: by directly measuring distances between atoms in compressed materials, it provides an unambiguous determination of material phase. Indeed, the time integrated x-ray diffraction (TarDIS [3]) platform at NIF has been used to collect high quality x-ray diffraction of materials (ramp) compressed to pressures as high as 20 Mbar [4], while searching for exciting new and predicted phases, such as electrides and carbon BC8.[5]

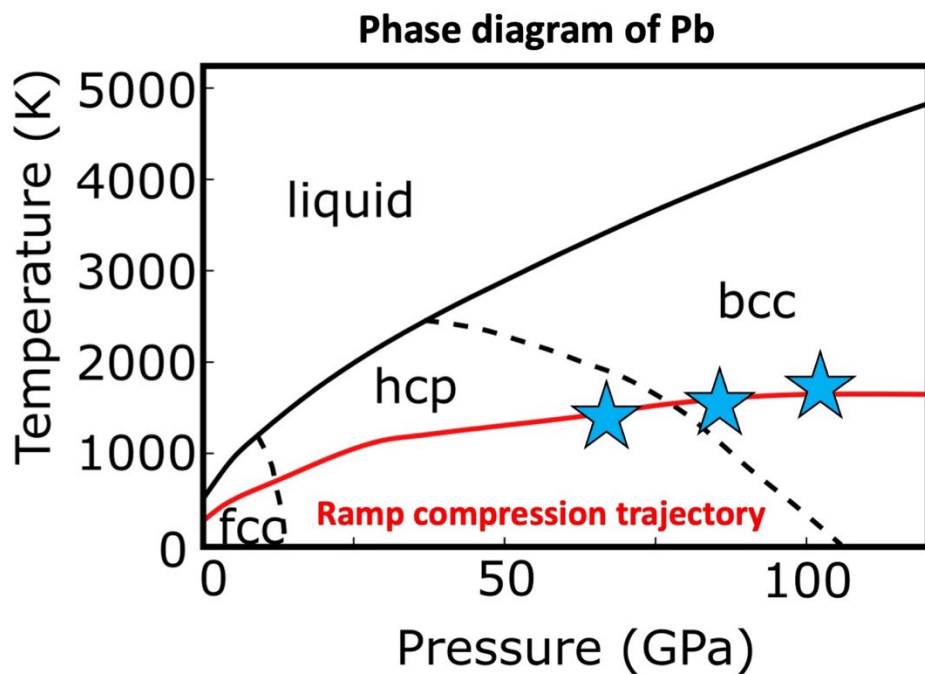


Figure2 Phase diagram of Pb in the region of pressure and temperature accessed in current NIF experiments. Our ramp compression trajectory crosses the predicted phase boundary between hcp and bcc structures. (Phase diagram from Smirnov 2021[6])

The development of an experimental platform to measure time-resolved x-ray diffraction at NIF is being undertaken to monitor phase transitions *as they happen* to understand how long transitions take to complete and to identify metastable and intermediate phases that may occur briefly during a phase transition. Moreover, it is anticipated that the ability to collect several diffraction measurements during a single laser experiment will not only maximize the data return for each expensive experiment but will provide important insights into the mechanisms that promote or hinder phase transitions. We are performing our development experiments on Pb, while it is ramp compressed 150 GPa, in order to observe a phase transition between the moderate-pressure hexagonally close packed phase (HCP) and the higher-pressure body centered cubic structure (BCC). The phase diagram of Pb (based on [6]) and our compression trajectory in thermodynamic phase space is shown in Figure 2.

The time-resolved x-ray diffraction experimental platform at NIF consists of the laser, a target assembly, and a diffraction diagnostic (see Figure 3). The target assembly holds the physics target containing the material of study, the backlighter that produces the x-ray source, and a mirror to direct VISAR light to the rear surface of the physics target. The target assembly also serves to shield the diffraction diagnostic from high-power unconverted infrared laser light and x-rays produced by the backlighter that are not used for diffraction. In this design we are limited to using the 96 beams in the lower half of NIF.

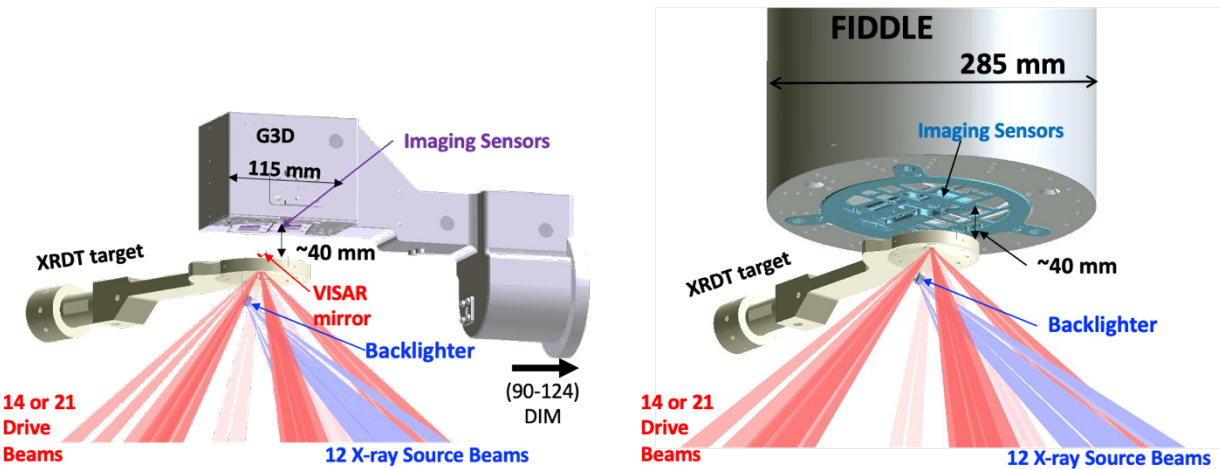


Figure 3. Time resolved x-ray diffraction platform at NIF (left) as fielded with the Gated Diffraction Development Diagnostic (G3D) and (right) as fielded with the Flexible Imaging Diffraction Diagnostic for Laser Experiments (FIDDLE).

In 2019 we built a prototype diagnostic (“G3D”) to assess the feasibility of directly collecting x-ray diffraction with electronic sensors (Figure 3, Left)[7]. This prototype was used to investigate the major risks to the diagnostics arising from EMI and Debris and Shrapnel generated from the laser matter interactions that created the drive on the sample and the x-rays from the backlighter target that provided the source for the x-ray diffraction. The prototype showed that both the EMI and debris and shrapnel could be controlled and multiple temporal frames could be obtained from a single experiment by using well shielded hCMOS detectors. This information fed into the design of a more sophisticated diagnostic that would have wider angular coverage and flexible configurations that would enable different materials to be studied with the minimum reconfiguration times. This diagnostic was called the FIDDLE: Flexible Imaging Diffraction Diagnostic for Laser Experiments. (Figure 3, Right). Both diagnostics use the same experimental platform (i.e., XRDT targets and lasers) to compress material to multi MBar pressures. In both configurations, the XRDT target has **four** functions: hold the physics package in position for the drive laser beams; hold the backlighter in position for the x-ray source laser beams; provide a first line of background shielding between the backlighter and the hCMOS sensors; and protect the G3D/FIDDLE from unconverted (infrared) laser light from NIF.

Development Experiments

FIDDLE is the culmination of several years of development work.

(1) We evaluated several possible experimental concepts, settling on direct detection to the Icarus[8]/Daedalus[9] family of hCMOS sensors as the most effective concept [10]. Direct detection is more efficient than any indirect methods, and it therefore should achieve higher quality x-ray diffraction than indirect methods with less heating of targets by the x-ray probe. The family of hCMOS sensors we have chosen are the fastest single-line-of-sight semiconductor imagers currently available, with the Icarus sensor able to collect 4 images, each integrating for 2ns, over a total of 14 ns. The Daedalus sensor will be able to collect 6 images (in zero-dead-time mode) over 12 ns. Moreover, any design should be compatible with future versions of the sensors that may be faster or otherwise improved.

(2) We built G3D, the development diagnostic to demonstrate that we could protect the delicate hCMOS sensors from the high-debris, high-EMP environment near the exploding target. We operated G3D on 15 NIF shots, during which we encountered and were able to solve several technical challenges e.g. EMI shielding, x-ray background reduction and debris and shrapnel mitigation). Also, as part of this demonstration work, we developed an experimental platform with an X-ray backscatter with a long duration (10 ns) [11]. This was required to create an x-ray source that lasts long enough to produce x-ray diffraction on each of the four imaging frames.

With G3D, we were able to demonstrate an x-ray diffraction measurement of Pb over four times as it was compressed through the phase transition from an hcp to a bcc crystal structure. Based on this result, we proceeded to design and build a more capable time-resolved x-ray diffraction diagnostic (FIDDLE).

While we consider the G3D results largely successful, the most important aspect of success was what we learned needed to be improved. Specifically:

- **Background mitigation:** With G3D we observed high backgrounds that lagged the x-ray source by 1-2 ns. Over the course of the 15 shots, we made substantial progress identifying and mitigating background sources, but we recognized that significant background reduction was still required to produce scientifically significant data.
- **Calibration and metrology:** Because G3D was a development diagnostic, designed merely to demonstrate that we could protect the sensors and collect diffraction data, we did not carefully metrologize the precise locations of the two Icarus sensors in G3D relative to each other and to the exterior surfaces /alignment fiducials of the G3D instrument. Nor did we carefully tune the two sensors we used to have identical operating frequencies and integration times. We found that the uncertainties resulting from these choices led to significant difficulties in analyzing the diffraction data that was collected.

- **Solid angle coverage and flexibility:** The two Icarus sensors we mounted in G3D were designed to be in the correct locations to document a specific phase transition and experimental configuration (Pb hcp – bcc at \sim 1Mbar with a 10keV Ge x-ray source). For different materials, pressures, and backscatterers, the location of important diffraction reflections will change. With our development experiments we did explore the idea of changing the backscatterer location or energy, a strategy that could be useful to “throw” diffraction to a specific place. However, we determined that strategy to be undesirable, both because it would reduce the ability to monitor the x-ray source intensity vs time and because it might change the background. Consequently, maximizing solid angle coverage and flexibility for diffraction measurement is critically important.

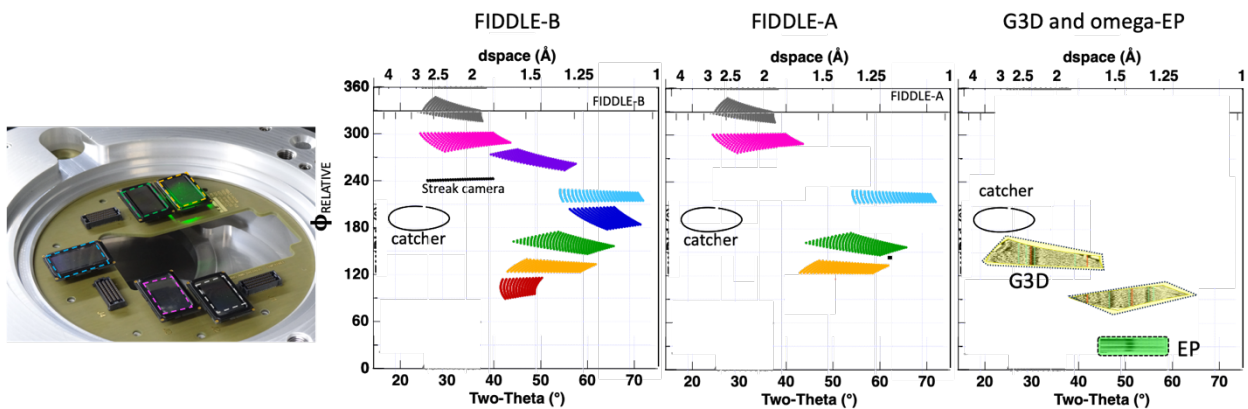


Figure 3. Diffraction phase space coverage with multiple sensors in FIDDLE compared to G3D and experiments at the Omega-EP laser. FIDDLE-A reflects the use of 5 Icarus sensors and a single available rotation. FIDDLE-B reflects the use of 8 Daedalus sensors along with an x-ray streak camera.

FIDDLE Design and Build

Having successfully demonstrated that direct detection is feasible, we turned our attention to the design and build of a robust experimental platform that will be able to make high-quality diffraction measurements for a wide variety of material transformations.

We intended to use as many lessons from the G3D development experiments as possible to minimize risk when fielding FIDDLE. We found that there were several new challenges involved in expanding the diagnostic to have greater functionality. The new challenges we encountered are summarized in Table 1.

The Final Design Review for FIDDLE-A was conducted in November 2022. The first iteration of the FIDDLE diagnostic is comprised of five Icarus sensors, due to delays in delivery of the faster Daedalus sensors. The next iteration of the diagnostic (FIDDLE-B) is expected to include eight Daedalus sensors as well as a streak camera to identify transitions that may be faster than the ns scale of the imaging sensors. FIDDLE-A was built and fielded on NIF in July 2023. FIDDLE-B is expected to be commissioned in FY25/FY26 depending on the data quality from FIDDLE-A.

Images of the FIDDLE-A design are compared with FIDDLE-B during build in Figure 4.

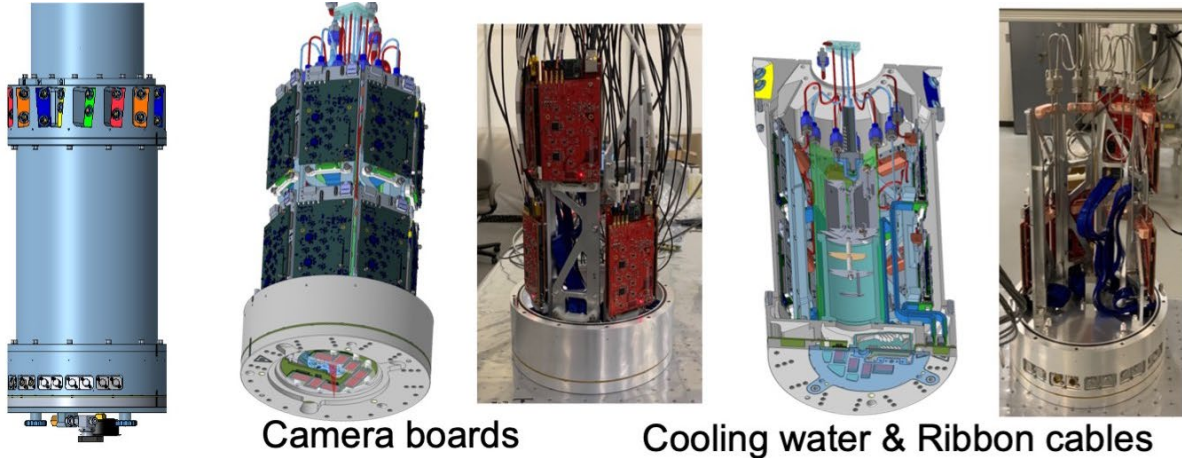


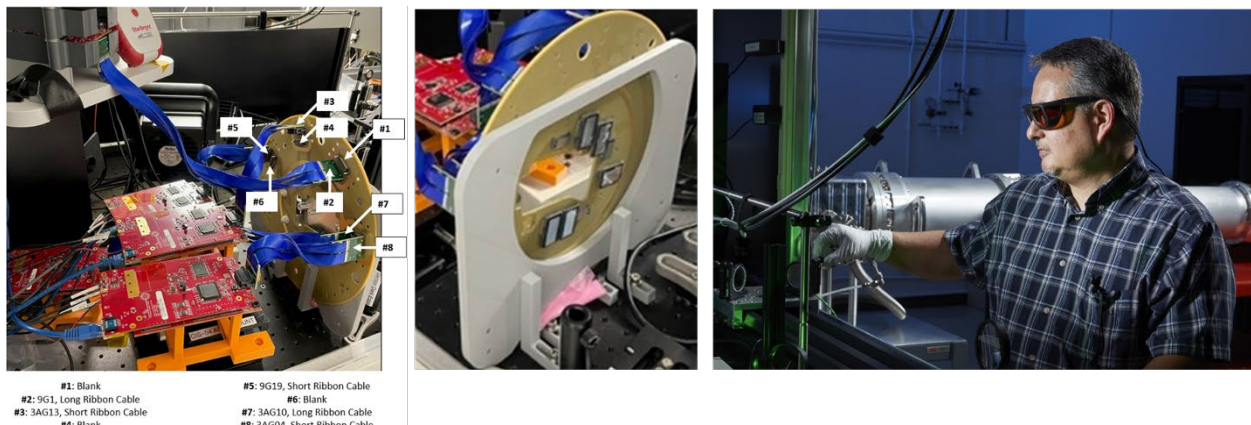
Figure 4. FIDDLE barrel during assembly compared to images from CAD model. ATLAS retroreflector locations along the top and bottom of the barrel were calibrated to ensure smooth alignment during shot operations.

Table 1. Design challenges encountered with FIDDLE that are new since G3D build

	Challenge	Design solution
Physics	Flexibility of diffraction location	8 sensors for maximum solid angle coverage Sensors installed on re-designable vacuum-feedthrough-circuit board Location in Polar DIM for rotational flexibility
	Need to perform multiple experiments for a single diagnostic cart install	Exchange front filters, image plates, and debris catcher in DIM
	Debris catcher geometry must be compatible with filter plate exchange	new debris catcher design + simulations
	Calibration and metrology	Sensor locations to be metrologized upon installation BEFORE primary electro-mechanical build. Sensors to be co-timed during characterization
Electrical	Eight sensors exceed maximum number of cables to Polar DIM	Innovative multiplexing and ethernet communications
	EMP: exchangeable front filter plate design created new EMP leaks to sensors	Aluminum EMP tape over EMI leak points for trouble shooting Front Filter Plate redesign in progress
Mechanical	Length, weight, and center of mass were initially beyond safety limits for a Polar-DIM mounted instrument	Minimize weight and moment arm with lightweight extension tube and custom shortened airbox.
	Debris wind to front filter plate	Maximize strength by minimizing apertures for time integrated diffraction and background assessment
	Thermal stability: 8 sensors + 8 camera boards + streak camera generates significant heat in a small volume	After thermo-mechanical analysis, added water cooling lines to each camera board and several fans inside Air Barrel

Diagnostic build proceeded in stages as calibration activities were performed on several subassemblies before they were integrated into the full FIDDLE.

First, the Icarus sensors underwent standard functional assessment and characterization (Figure 5) before they were installed onto the vacuum feed-through board and the diagnostic head. (Figure 6) The precise location and orientation of each sensor was then metrologized relative to the center of the FIDDLE barrel using a coordinate-measurement-machine (CMM). When analyzing data from G3D, we learned that knowledge of the relative location between sensors to within 100 μ m is required. The precision measurements from the CMM shop are significantly better than the 100 μ m requirement.



Next, the air-barrel was assembled as camera boards, ribbon cables, and cooling water lines were installed (Figure 7). At this stage, the locations of the ATLAS (alignment features) retroreflectors on the air-barrel subassembly were calibrated at the snout characterization station in the Target Diagnostics Factory to ensure that the diagnostic alignment plan could proceed successfully.



Figure 7. FIDDLE barrel in build after CMM metrology. Right. Barrel in Target Diagnostic “Factory” snout alignment calibration station.

Finally, the airbox was assembled, connecting all sensors, electronic monitors, and cooling water to a standard airbox interface. (Figure 8) Electronic multiplexing was required to communicate with all sensors through the limited number of cables in the polar dim.



Figure 8. FIDDLE airbox in build after calibration of the barrel in the TD Factory

Once all electronics were installed, including the serialized cables that would be connected to NIF infrastructure, the entire FIDDLE was returned to the laser lab for final timing. The five sensors were adjusted to trigger at the same time (within ± 100 ps) by manually cutting the trigger cables to each sensor.

Prior to participating on a NIF shot, we also developed software to enable shot setup and full ICCS integration of FIDDLE. Pre-shot commissioning in NIF also included installation in the polar DIM, including an activity to install and exchange the FIDDLE front-filter-plate, which serves a similar function to a snout on many other dim diagnostics and is exchanged in the DIM between shots.

Commissioning FIDDLE on NIF

FIDDLE has been deployed at NIF for four shots: N230727-001, N230928-001, N231116-001, and N240215-002. On the first shot, N230727-001, all Icarus sensors were saturated, and the multiplexed timing monitors showed large jumps in time on the system shot relative to the pre-shot dry-runs. After some investigation, it was determined that these phenomena were related to EMI leaks in the front portion of the FIDDLE diagnostic.

To learn more about the EMP/EMI levels within the detector a B-dot probe was installed inside FIDDLE to monitor EMP near the Icarus sensors. It showed significantly higher voltage than

similar shots with G3D. Several locations of EMI leakage were identified in the TD factory using a network analyzer to send a signal to the internal B-dot probe that could be detected outside of FIDDLE wherever the shielding was imperfect. As a test, those locations were covered with EMI-shielding Aluminum tape. With the tape in place, no EMI leakage was observable in the TD factory experimental setup, so the tape-shielded FIDDLE was fielded on shot N240215-002 to confirm that the EMI leak was the origin of the saturated detectors and timing jumps.

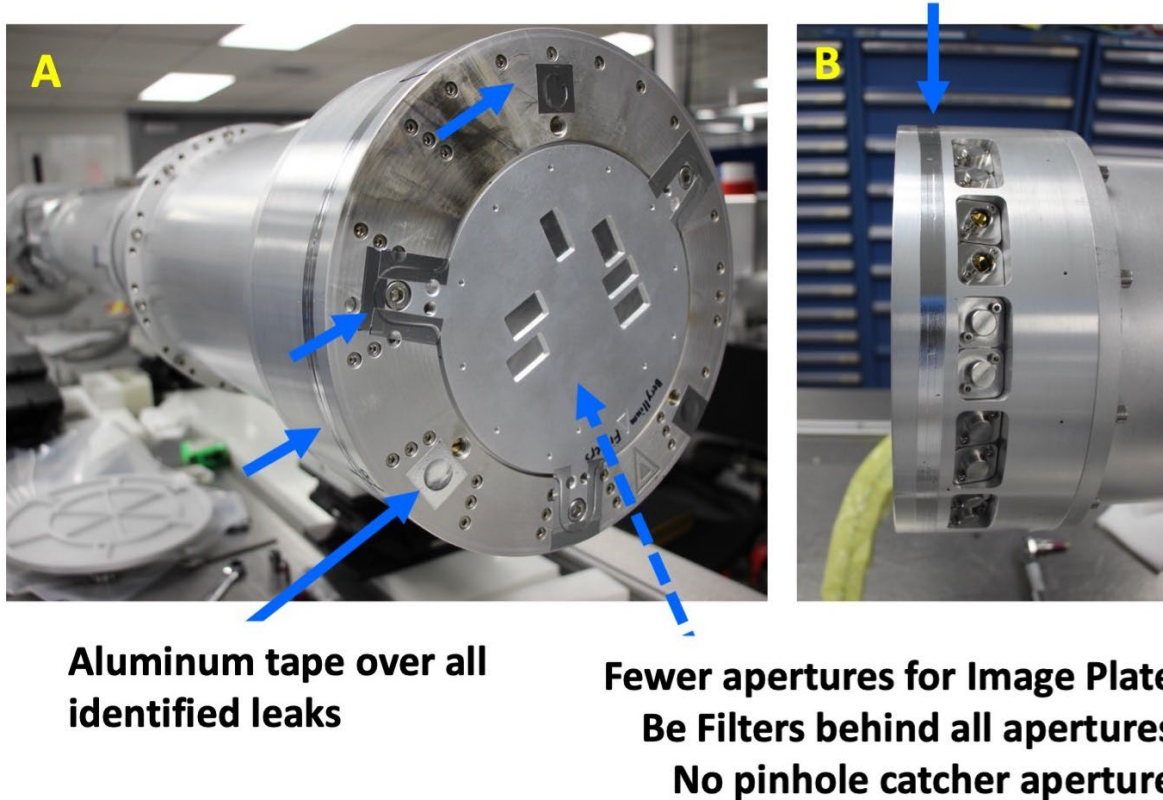


Figure 9 EMP mitigation test in FIDDLE front end. FIDDLE Front (A) and Side (B) views showing EMI shielding with Aluminum tape (Blue arrows) that was added for shot N240215-002. For additional EMP shielding, the number of apertures in the front filter plate was reduced, and the area behind each sensor was shielded with 500 μ m of Beryllium (dashed arrow).

Indeed, EMP observed with the B-dot probe during the NIF shot was reduced significantly by the application of the aluminum tape-shielding (Figure 10). Moreover, and consistent with our prior assessment that the problems observed in the image data were the result of EMP, N240215-002 was the first shot on which all five Icarus cameras operated as expected: triggering at or near the requested time and collecting x-rays with no evidence for high non-x-ray background. The image data for shot N240215 is shown in Figure 11.

Plotting the diffraction data from Sensor 7 in diffraction space (also called “polar view”) helps confirm that the observations are diffraction. In this view diffraction angles ($\phi, 2\theta$) within each sensor image are calculated based on the designed location of the sensor relative to the physics

target. When images are plotted in this space (I.e., as Intensity vs $(\phi, 2\theta)$) diffraction manifests as intensity at constant 2θ , or a vertical line. In Figure 12, the first 3 frames of Sensor 7 are plotted in polar view and the observed (vertical) diffraction lines are indicated with red arrows.

In addition to the improved EMP shielding, diffraction quality (signal-over-background) was also improved between shots by adding low-Z shielding to the surfaces of the target that are visible to FIDDLE. It is hypothesized that a significant source of background is x-ray emission caused by hot electrons striking the top and sides of the XRDT target. When hot electrons impact matter, bremsstrahlung emission x-rays are emitted in proportion to the atomic number of the material that absorbs the electrons. Thus, one strategy for reducing x-ray emission is to reduce the Z of the material impacted by electrons.

In Figure 13, image plate data in a single aperture is shown for three of the four FIDDLE shots. (N231116 is omitted because one of the 3 quads of backlighter was dropped, so the data is not simple to compare). From shot-to-shot, small additions were added to the target in an effort to reduce background. Specifically, the stainless steel and Tantalum-Tungsten (TaW) components were covered with aluminum ($Z=16$), and later that aluminum was further coated with parylene (CH , $Z \sim 6$). With each of these low-Z additions, background measured on image plate aperture 6 was reduced by approximately 50 %.

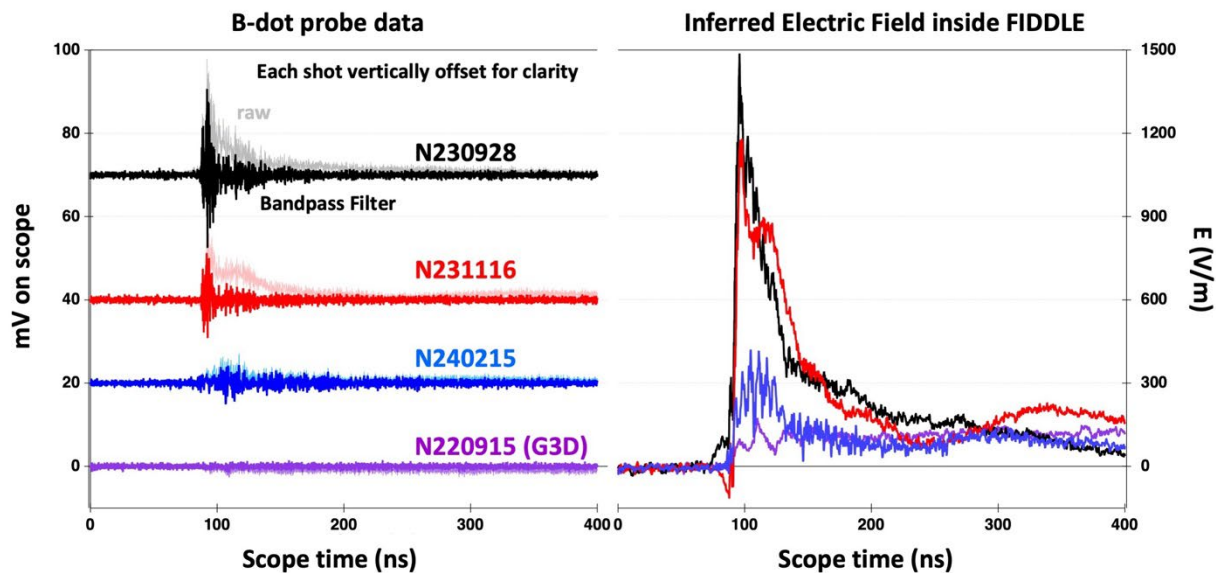


Figure 10 EMP mitigation effectiveness demonstrated with B-dot probe inside the FIDDLE diagnostic. **Left** Raw and bandpass-filtered B-dot probe signal. **Right** Inferred electric field inside FIDDLE (integral of B-dot signal). EMP inside fiddle was slightly reduced between shot N230928 and N231116 by improving the conductive epoxy seal at the first Aluminum filter. EMP inside fiddle was significantly reduced between shot N231116 and N240215 by adding the aluminum tape and reducing apertures as shown in figure 9. In all cases, EMP is still higher than was observed inside G3D for a similar shot.

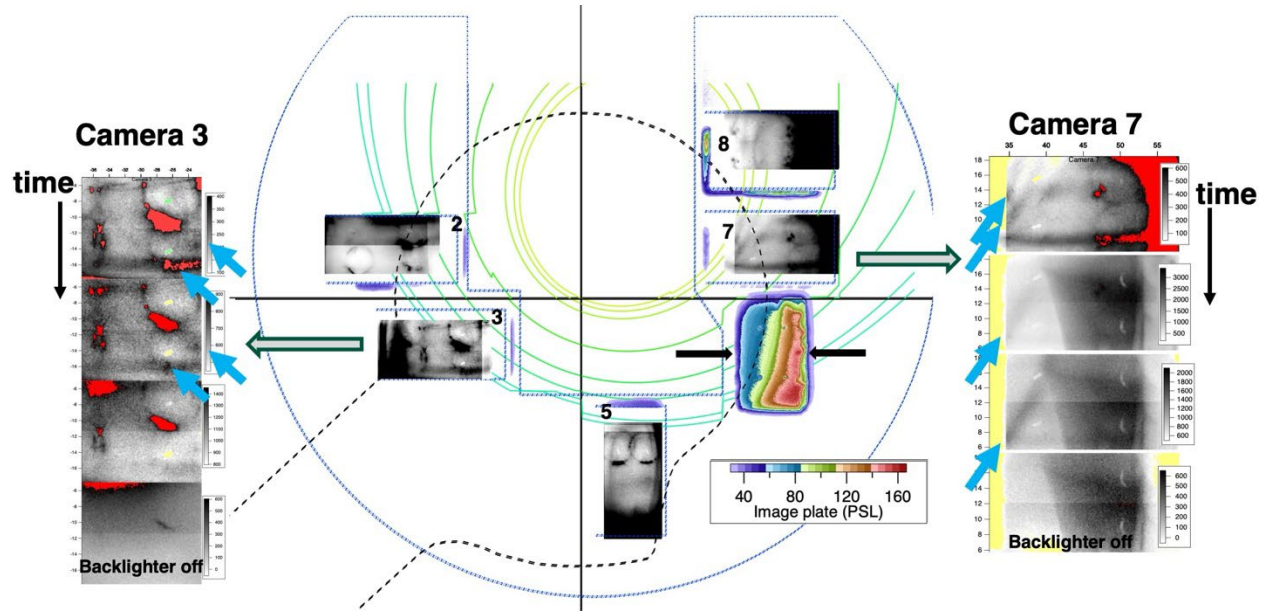


Figure 11 FIDDLE image data from shot N240215-002. The first frame of each sensor (gray scale) and the image plate data (color scale) are shown in their actual locations in a coordinate system based on the FIDDLE image plate scan direction. Contours are shown where diffraction of Pb is expected. The four time-dependent frames of camera 3 and camera 7 are shown at the sides of the figure, with arrows pointing to data that we believe is x-ray diffraction. The fourth frame of each sensor collected data after the backlighter (x-ray source) was off, so no diffraction was expected in the last frame. The image plate data (colored portion of image) is used to monitor and compare x-ray background levels. The black arrows at the image plate indicate the location of the lineout shown in Figure 13.

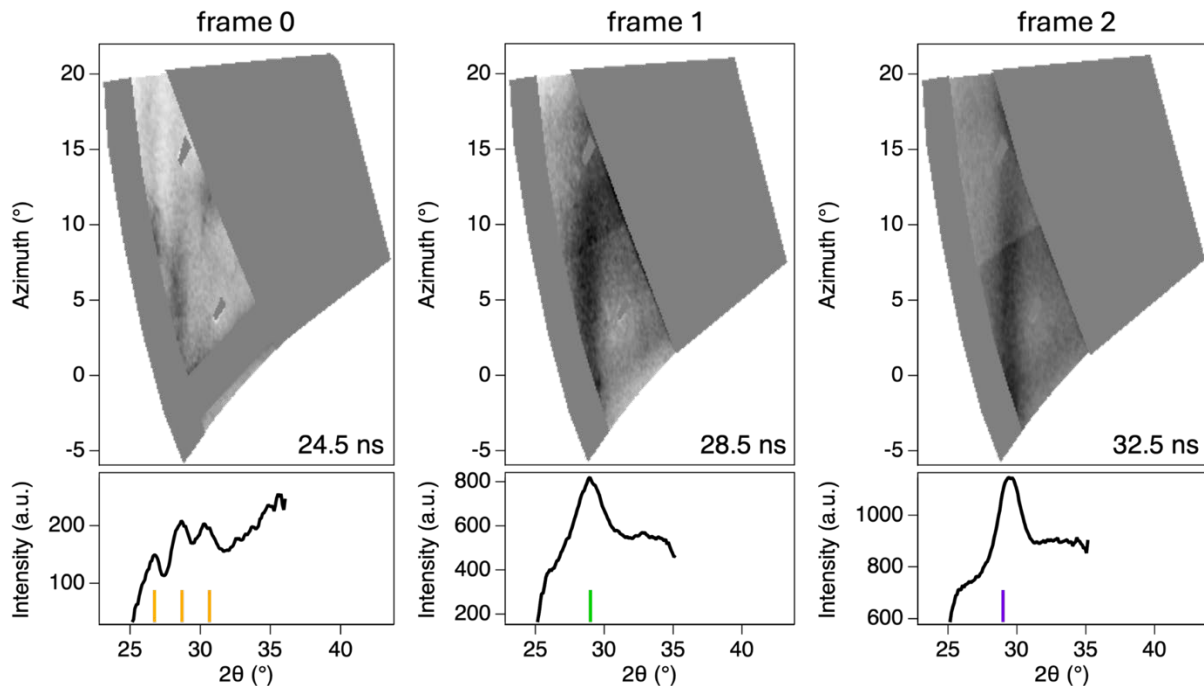


Figure 12 Polar view of Sensor 7 images shows diffraction clearly. The diffraction pattern in frame 0 is consistent with HCP Pb, while the pattern in frame 2 indicates the presence of BCC Pb.

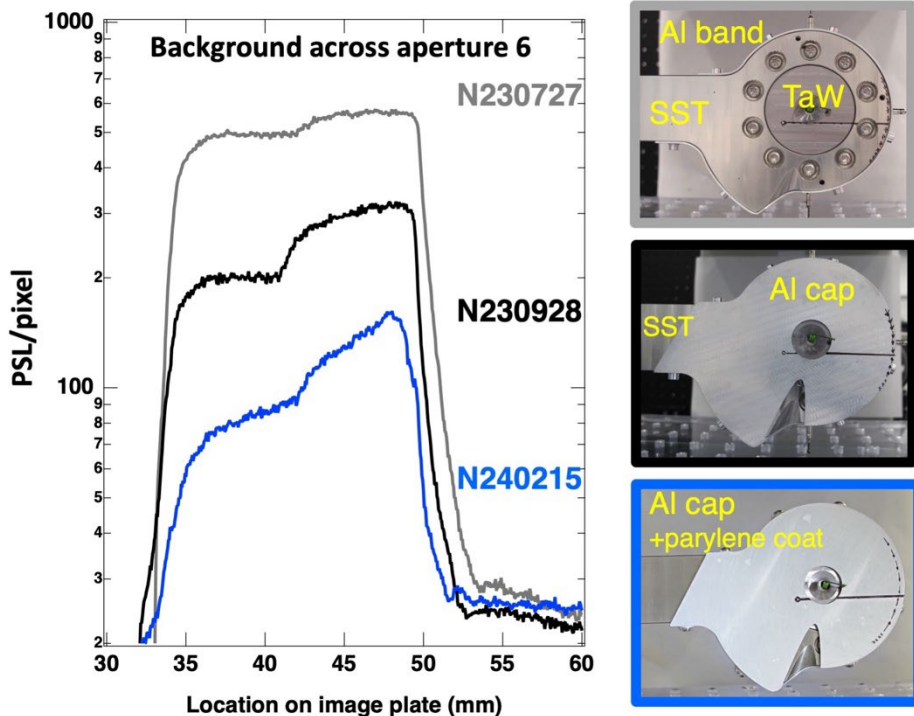


Figure 13. Background Reduction due to target shielding. (Left) Image plate signal across aperture 6 for three NIF shots with increasing low-Z shielding. (Right) Top view of the XRDT target for each shot showing the shielding to reduce x-ray emission when hot electrons strike the target by reducing the effective atomic number of the material that absorbs the electrons.

Lessons Learned with FIDDLE:

EMP shielding. In order to add the additional flexibility to perform multiple shots with a single DIM-cart install and with a variety of targets, the front-most elements of FIDDLE were designed to be different than the development diagnostic (G3D). Although we were aware that EMP was an important issue, the relatively low levels of EMP/EMI with G3D meant that we did not give enough consideration to changes to EMP caused by the design changes between G3D and FIDDLE. EMP is not straightforward to model or measure and this resulted in the team underestimating the effect of EMP on the new FIDDLE design.

We have learned that it is important to be vigilant in assessing susceptibility to electromagnetic interactions with each small design change. Using a network analyzer to search for EMP leaks in the instrument was suggested by an EMP expert, and it was critical to the success of the project. Building up expertise in the area of EMP/EMI is important to understand going forwards and this will be built into planning of future upgrades to FIDDLE and similar diagnostics.

.

Multiplexing. While multiplexing was necessary to satisfy the cabling challenges, it also turned out to be susceptible to EMP-induced noise.

The LLNL-designed v4 camera boards require two triggers and produce two monitors for each sensor. One edge detect monitor signal picks off a triggering step voltage at one corner of the sensor, and one oscillator monitor reads a divided-by-16 monitor of the 500 MHz oscillator voltage. We use those two monitors to confirm the on-shot camera trigger time and operating frequency. However, the polar DIM infrastructure does not support enough cables for us to independently trigger and monitor all 8 sensors in FIDDLE. Consequently, in this constrained environment, we implemented a design that reduced the 32 signals to 7: one coarse trigger for all 8 sensors, two fine triggers, two multiplexed oscillator monitors and two multiplexed trigger monitors.

Each multiplexed monitor combines 4 monitors into one signal by processing the signal with an internal logic board (integrated circuit). Each trigger's voltage jump is automatically detected and replaced with a 75 ns "on" signal so that 4 triggers can be combined. Similarly, the oscillator monitor is detected and truncated so that the four sets of oscillations can be measured with a single voltage trace.

We tested the multiplexing circuit extensively before and during the FIDDLE build and found it to effectively transmit the sensor timing. However, the monitor signals did not behave correctly on our actual NIF shots, and timings were inferred to be tens of ns different from the intended timing.

We were not able to fully identify what was happening to our multiplexed timing circuit until we added additional cabling to the circuit to directly sample a few of the monitor voltages (using cables otherwise reserved for future capabilities). We eventually determined that the monitor signals were significantly noisier during NIF shots than they were on dry runs before or after the shot and that the noise was affecting the timing determination by the internal logic circuit. We inferred that this noise was due to on-shot EMP leaking into FIDDLE.

While we anticipate that additional EMP shielding will reduce noise to the circuit, we are also redesigning the multiplexing circuit to be significantly more robust to noise. We will also continue to compare at least one direct voltage monitor to the processed monitor until we have increased confidence in the new timing circuit.

It is important to note the difference between a multiplexing strategy that merely delays and combines signals without information loss (as is used in the x-ray framing cameras at NIF) with one that uses logic to process signals inside the instrument (as is used in FIDDLE). By not preserving the full analog voltage signal picked off from each sensor, we lost valuable information about unintended voltage variations at the sensor. In an ideal world we would preserve all possible information from each sensor, but as that is not always possible, it is critical to design the multiplexing circuitry with care and to be mindful of the circuit's limitations when interpreting data.

Catcher geometry. We successfully fielded shot N240215 without a dedicated vessel to catch the accelerated pinhole. Instead, we simply covered the nominal catcher aperture with the 2.5 mm thick aluminum of the front filter plate frame. While this off normal geometry was accommodated primarily to allow us to minimize openings through which EMP might leak into FIDDLE, it also effectively demonstrated that in many cases, the catcher may not be necessary to protect the instrument from damage due to debris. (It may still be critical for higher drive energies or to contain hazardous materials.)

In this first design of FIDDLE, the catcher occupies a significant fraction of the useful diffraction space. If future versions of FIDDLE can be redesigned with a much smaller catcher (or none at all), diffraction data quality may be significantly improved. We further anticipate careful reconsideration of the requirements for catching (including catching hazardous materials) in future iterations of FIDDLE.

Background reduction will continue to be of paramount importance in the commissioning and development of FIDDLE. Upcoming shots with FIDDLE are intended to document alignment accuracy and repeatability, timing precision, and EMP reduction. As we document these accuracies, many of which have been made possible with our improvements in metrology and calibration, we anticipate that the largest remaining challenge to data quality will be x-ray background.

FIDDLE is intended to be used primarily to document phase transitions. To do that, diffraction intensity must be measurable and accurate as the phase fraction changes, *i.e.*, when diffraction intensities are strong and also when they are weak. The biggest challenge to identification and quantification of weak diffraction lines will be the level of x-ray background on the sensors. Thus we must anticipate that background identification, reduction, and mitigation will be an integral part of the FIDDLE development program for the next several years so this will be the focus of future development efforts for this experimental platform.

Conclusion & Future Plans

FIDDLE will be fielded once more in FY24, and we aim to demonstrate continued reduction of EMP leakage into FIDDLE as well as additional background reduction by further improved target shielding. We will continue to field FIDDLE in FY25 with the aim of improving diffraction signal quality to a level that will be useful to the Materials HED Program. We anticipate primarily improving data quality by continued background reduction along with additional calibration activities to assess the uncertainty of diffraction timing, angles, and intensities.

A future phase of development, called FIDDLE B, is planned to provide improved angular coverage and improved sensors without introducing new EMP/EMI or x-ray background sources. Currently we envision that FIDDLE B will include:

- 8 Daedalus sensors
- Addition of x-ray streak camera
- Reduced area for debris catching

- Additional area to collect x-ray diffraction at relevant diffraction angles, and
- Improved EMP shielding.

Most critically, FIDDLE B will incorporate a new front end that is still designed to be easily exchanged in the DIM but that also effectively shields EMP.

The Daedalus sensors should offer three clear benefits over the current set of Icarus sensors. First, with their different packaging, we will be able to fit 8 sensors onto the vacuum feed through circuit board instead of the 5 Icarus currently in FIDDLE. Second, the sensor itself should be faster, with integration times <2ns and possibly nearing 1ns. Finally, the zero-dead-time pixel interlacing mode will enable 6 frames of continuous measurement, increasing the temporal resolution without loss of imaging range.

The addition of an x-ray streak camera to capture a small range of diffraction angles with high temporal resolution (10-30 ps) is very important to our key user community as it will allow us to assess if transitions are happening faster than our imaging sensors can measure them and thus to develop requirements for future diffraction measurements.

We anticipate that FIDDLE-B development will begin in FY25. Beyond FIDDLE-B, future plans also include a need to enable classified operations. However, as classified operations protocols would not be compatible with the use of a B-dot probe to monitor EMP, we must first be certain that the EMP problem is solved. Finally, We also plan to enable rotation of FIDDLE in the DIM for additional shot-to-shot flexibility to support a wide variety of FIDDLE experiments.

References

- [1] M. G. Gorman, *et al.*, “Experimental observation of open structures in elemental magnesium at terapascal pressures,” *Nat. Phys.* **18**(11), 1307–1311 (2022). doi.org/10.1038/s41567-022-01732-7
- [2] R. G. Kraus, *et al.*, “Melting of Tantalum at Multimegabar Pressures on the Nanosecond Timescale,” *Phys. Rev. Lett.* **126**, 255701 (2021). doi.org/10.1103/PhysRevLett.126.255701
- [3] J. R. Rygg, *et al.*, “X-Ray diffraction at the national ignition facility,” *Rev. Sci. Instrum.* **91**(4), 043902 (2020). doi.org/10.1063/1.5129698
- [4] Lazicki, A., *et al.*, Metastability of diamond ramp-compressed to 2 terapascals. *Nature* **589**, 532–535 (2021). doi.org/10.1038/s41586-020-03140-4
- [5] D. N. Polsin, *et al.*, “Structural complexity in ramp-compressed sodium to 480 GPa,” *Nat. Commun.* **13**(1), 2534 (2022). doi.org/10.1038/s41467-022-29813-4

[6] N. A. Smirnov, "Ab initio calculations of the phase diagrams of tin and lead under pressures up to a few TPa," *J. Phys.: Condens. Matter* **33**, 035402 (2021). doi.org/10.1088/1361-648X/abbbc5

[7] K. Werellapatha, *et al.*, "Time-resolved X-ray diffraction diagnostic development for the National Ignition Facility," *Rev. Sci. Instrum.* **95**, 013903 (2024). doi.org/[10.1063/5.0161343](https://doi.org/10.1063/5.0161343)

[8] L. Claus, *et al.*, "Design and characterization of an improved, 2 ns, multi-frame imager for the Ultra-Fast X-ray Imager (UXI) program at Sandia National Laboratories," *SPIE Proceedings*, **10390**, Target Diagnostics Physics and Engineering for Inertial Confinement Fusion VI; 103900A (2017)). doi.org/[10.1117/12.2275293](https://doi.org/10.1117/12.2275293)

[9] L. Claus, *et al.*, "Design and characterization of a novel 1-ns multi-frame imager for the Ultra-Fast X-ray Imager (UXI) program at Sandia National Laboratories," *SPIE Proceedings*, **10763**, Radiation Detectors in Medicine, Industry, and National Security XIX; 107630M (2018). doi.org/[10.1117/12.2319856](https://doi.org/10.1117/12.2319856)

[10] L. R. Benedetti, *et al.*, "Conceptual design for time-resolved x-ray diffraction in a single laser-driven compression experiment," *AIP Conference Proceedings* **1979**, 160004 (2018). doi.org/10.1063/1.5045003

[11] K. Werellapatha, *et al.*, "Long duration x-ray source development for x-ray diffraction at the National Ignition Facility," *Rev. Sci. Instrum.* **92**, 053904 (2021). doi.org/10.1063/5.0043677